Pressure-induced quantum phase transition in the quantum antiferromagnet CsFeCl3

Shohei Hayashida,[1] Oksana Zaharko,[2] Nobuyuki Kurita,[3] Hidekazu Tanaka,[3] Masato Hagihala,[1] Minoru Soda,[1] Shinichi Itoh,[4] Yoshiya Uwatoko,[1] and Takatsugu Masuda[1]

[1]*Institute for Solid State Physics, The University of Tokyo, Chiba 277-8581, Japan*
[2]*Laboratory for Neutron Scattering and Imaging, Paul Scherrer Institut, CH-5232 Villigen, Switzerland*
[3]*Department of Physics, Tokyo Institute of Technology, Meguro-ku, Tokyo 152-8551, Japan*
[4]*Neutron Science Division, Institute of Materials Structure Science, High Energy Accelerator Research Organization,*
Tsukuba, Ibraki 305-0801, Japan

We have studied the pressure-induced quantum phase transition in the singlet-ground-state antiferromagnet CsFeCl3. Neutron diffraction experiments under pressure evidence the magnetic long-range order at low temperatures. Magnetic structure analysis reveals a 120° structure with a propagation vector of $k_{mag} = (1/3,1/3,0)$. The estimated critical exponent of the order parameter suggests that CsFeCl3 belongs to the universality class of $U(1) \times Z_2$ symmetry which is expected to realize the chiral liquid state.

Quantum phase transition (QPT) rooted in the quantum uncertainty between kinetic and potential energies has been a central topic of condensed-matter physics. The extent of the quantum fluctuation determines the ground state to be or not to be ordered, and it is controlled by external parameters such as pressure, magnetic field, and chemical doping [1,2]. One has a chance to observe an exotic phenomenon in the vicinity of the quantum critical point (QCP) in which the effect of the quantum fluctuation is enhanced. To date the QPT has provided unsolved puzzles in many condensed-matter systems including quantum spin systems [3,4], high-temperature superconductors [5–8], heavy fermion metals [9,10], two-dimensional electron systems [11], and ultracold atom systems [12,13].

The importance of the quantum spin system is an easy access to the verification of experiments and theories. For instance, in the spin-dimer compound TlCuCl3, the QPTs induced by the magnetic field [14,15] and the pressure [16–19] have been observed. These experimental works have triggered many theoretical studies: the interpretation of the field-induced order as the Bose-Einstein condensation of magnons [20–22], the Higgs mode near the QCP [23,24], and universality in three-dimensional (3D) quantum antiferromagnets (AFs) [25–29]. The spin system is thus a good playground for the study of the QPT.

The spin $S = 1$ AF of easy-plane type is one of the simplest systems exhibiting the QPT. The Hamiltonian is expressed by

$$\mathcal{H} = \sum_i D(S_i^z)^2 + \sum_{ij} J_{ij} \boldsymbol{S}_i \cdot \boldsymbol{S}_j, \qquad (1)$$

where $\boldsymbol{S}_i$ is a spin operator at the ith site. The easy-plane anisotropy D splits the triplet spin $S = 1$ into the singlet $S^z = 0$ and the doublet $S^z = \pm 1$ as shown in Fig. 1(a), favoring the disordered singlet ground state. In contrast, the spin interaction J_{ij} favors a magnetic order. Control of the competition between the anisotropy and the spin interaction by an external parameter brings about the QPT. Recent theories

predict nontrivial phenomena near the QCP: an enhanced longitudinal magnon in the tetragonal lattice [30] and the appearance of the chiral liquid state in the triangular lattice [31]. From the viewpoint of experiment, hydrostatic pressure is a good external parameter since it tunes the spin interaction and anisotropy with the system symmetry unchanged. It is noted that applying magnetic field lowers the symmetry and chemical doping induces randomness. Nevertheless, pressure-induced QPT has not been experimentally studied in the easy-plane type AF having the singlet ground state.

CsFeCl3 is a singlet-ground-state AF where Fe^{2+} ions ($3d^6$, $S = 2$, $L = 2$) are responsible for the magnetism. The FeCl6 octahedra form a one-dimensional chain along the crystallographic c axis as shown in Fig. 1(b), and the chains form the triangular lattice in the ab plane in Fig. 1(c) [32]. The low-energy excitation of the Fe^{2+} ion is described by a pseudospin $s = 1$ due to the cubic crystal field and spin-orbit coupling. Moreover, the pseudospin is split into $s^z = 0$ singlet ground state and $s^z = \pm 1$ doublet state caused by the easy-plane type single-ion anisotropy $D(s^z)^2$. Inelastic neutron scattering experiments identified the spin system as the ferromagnetic chain which is weakly coupled by the antiferromagnetic interaction in the triangular plane [33]. Combination of the low dimensionality and the strong easy-plane-type anisotropy favors the quantum singlet ground state. Indeed, the magnetic order was not observed at low temperatures [34].

Very recently, the magnetic susceptibility measurement exhibited a pressure-induced magnetic transition at a low temperature [35]. The result indicated that applying pressure effectively enhanced the spin interaction, suppressed the anisotropy gap, and induced a QPT. CsFeCl3 is thus a good model compound for the pressure-induced QPT in the spin $S = 1$ singlet-ground-state AF. It is of primary importance to identify the magnetic structure and to discuss the universality class of the pressure-induced ordered phase in CsFeCl3.

A single-crystal sample was grown by the vertical Bridgman method [35]. The crystal with the mass of 0.20 g was put in a
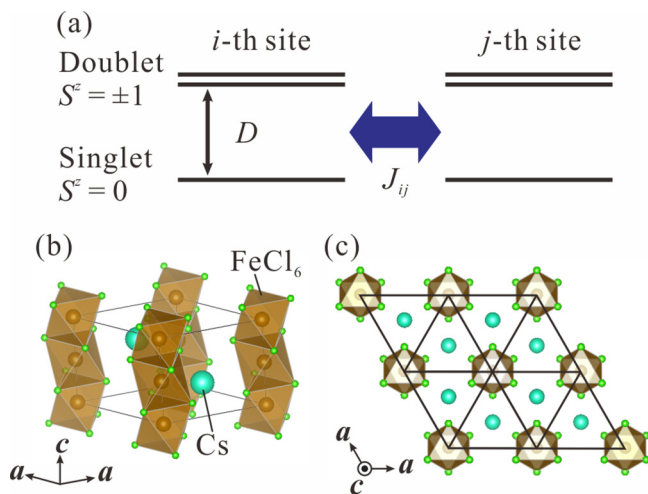
FIG. 1. (a) Schematic diagram of local energy scheme and intersite interaction. (b) Perspective view of the crystal structures of $CsFeCl_3$ with the space group $P6_3/mmc$. (c) Triangular lattice in $CsFeCl_3$.
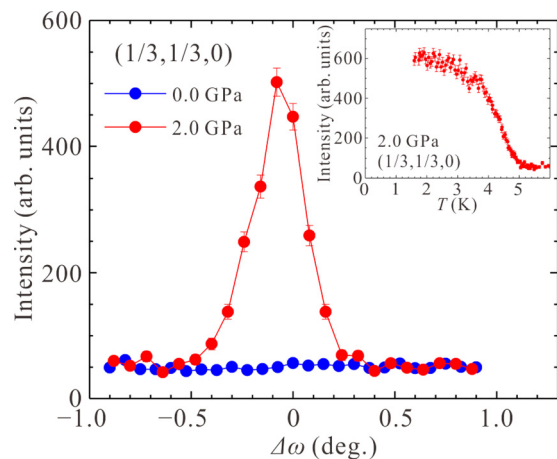

FIG. 2. The ω scans for $(1/3,1/3,0)$ reflection measured at $T = 1.6$ K. The blue and red circles are data at 0.0 and 2.0 GPa, respectively. The inset is the temperature dependence of the magnetic Bragg peak intensity for $(1/3,1/3,0)$ reflection measured at 2.0 GPa.

Teflon cell with a deuterated glycerin as a pressure medium. The crystal was mounted so that the horizontal plane was the ab plane. The Teflon cell was installed in a piston-cylinder clamped cell made of Al alloy. The pressure-induced magnetic order was observed by a preliminary neutron Laue diffraction measured at the high-resolution chopper spectrometer (HRC) in J-PARC/MLF, Japan. Then neutron diffraction experiments under pressures were performed at the single-crystal neutron diffractometer ZEBRA at the Swiss Neutron Spallation Source, Paul Scherrer Institut (PSI) in Switzerland. A ^{4}He cryostat was used to achieve the base temperature of 1.6 K. A Ge(311) monochromator was chosen to obtain the neutrons with the wavelength of 1.178 Å. In addition to the in-plane reflections of $(h,k,0)$, the out-of-plane reflections of $(h,k,\pm1)$ were collected by using the lifting counter of ZEBRA. The data were analyzed by the Rietveld method using FULLPROF software [36]. Candidates for the magnetic structure compatible with the lattice symmetry were obtained by the SARA*h* software [37].

The ω scans at $\boldsymbol{Q} = (1/3,1/3,0)$ reflection measured at 1.6 K for $P = 0.0$ and 2.0 GPa are shown in Fig. 2. A new peak is induced by applying pressure. Its intensity increases with the decrease of the temperature below 5 K as shown in the inset of Fig. 2, which means that the peak is magnetic. The magnetic Bragg peaks are observed in $(h \pm 1/3, k \pm 1/3, 0)$, leading to the magnetic propagation vector of $\boldsymbol{k}_{mag} = (1/3,1/3,0)$.

The nuclear Bragg peaks at each pressure and at the base temperature are reasonably fitted by the hexagonal structure with the space group $P6_3/mmc$ which was previously reported for the room temperature [32]. The R_F factors for 1.4, 1.6, 1.8, 2.0, and 2.2 GPa are 8.2, 4.5, 3.8, 13.2, and 5.2%. We can thus safely assume that the crystal structure with the space group $P6_3/mmc$ is retained at each pressure in the magnetic structure analysis. In the representation analysis, the space group $P6_3/mmc$ and the magnetic propagation vector $\boldsymbol{k}_{mag} = (1/3,1/3,0)$ lead to four irreducible representations $\Gamma_3 + \Gamma_4 + \Gamma_5 + \Gamma_6$. The basis vectors for Γ_3 and Γ_4 exhibit the easy-axis type structures with the magnetic moments along the

c axis in which the moments are modulated by the propagation vector. The basis vectors for Γ_5 and Γ_6 exhibit 120° structures in the ab plane. The relations of the neighboring moments along the c axis are ferromagnetic for Γ_3 and Γ_6, and those are antiferromagnetic for Γ_4 and Γ_5.

The magnetic Bragg peaks are observed in the case of $l = 0$ and not in the case of $l = 1$ as listed in Table I, which means that the alignment of the moments along the c axis is ferromagnetic. Then the models of Γ_4 and Γ_5 are excluded. Calculated neutron intensities at the $l = 0$ reflections for Γ_3 and Γ_6 are the same. Consider that $CsFeCl_3$ has the easy-plane type anisotropy, the model of the Γ_3 exhibiting easy-axis type structure is not reasonable, and the model of the Γ_6 is selected. As the result of the Rietveld refinement in Fig. 3, the structure for Γ_6 gives a good agreement with the experimental data. The magnetic moments therefore form the 120° structure in the ab plane, and ferromagnetically propagate along the c axis as shown in the inset of Fig. 3. The refined magnitude of the moment and refinement factor for each pressure are listed in Table II.

To discuss the universality class of the pressure-induced ordered phase, we estimate the critical exponent of the order parameter. Unlike a typical second-order transition, the order parameter exhibits a broad transition as shown in the inset of Fig. 2. We presume that the inhomogeneity of the pressure leads to the distribution of the transition temperature T_N [38–41]. Then the temperature dependence of the magnetic peak is

TABLE I. Integrated intensities of the magnetic Bragg peaks at 1.6 K and at 2.0 GPa.

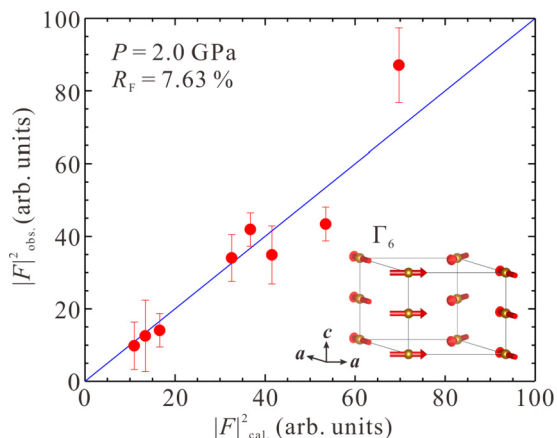| (h,k,l)	$|F|^2$ (arb. units)
$(1/3,1/3,0)$	87.06
$(2/3,2/3,0)$	43.39
$(4/3,-1/3,0)$	41.88
$(1/3,1/3,1)$	0
$(2/3,2/3,1)$	0
$(4/3,-1/3,1)$	0

FIG. 3. Magnetic structure factors measured at 1.6 K and at 2.0 GPa plotted against those obtained by the model calculation for Γ_6. The inset is an example of the magnetic structure for Γ_6.

expressed by

$$I(T) = I_0 + A\sqrt{\frac{4\ln(2)}{\pi \Delta T_N^2}} \int \exp\left(-4\ln(2)\frac{(\tau - T_N)^2}{\Delta T_N^2}\right)$$
$$\times (\tau - T)^{2\beta} d\tau, \qquad (2)$$

where I_0 is offset, A is the scaling factor of the intensity, ΔT_N is the fluctuation of T_N, and β is the critical exponent. ΔT_N is fixed to be 0.4 K, since the accuracy of applying pressure is ± 0.1 GPa and the T_N shifts by 0.4 K with the change of 0.1 GPa in the pressure-temperature phase diagram [35]. We perform the fitting to the data at 2.2 GPa because the T_N is the highest and the number of data points is the most among the measured pressures. The data in the range of 4.5 K $< T <$ 7.0 K are used for the fit, where the I_0 is evaluated from the high-temperature data. Fitting parameters are T_N, A, and β. As a result of the fitting, the transition temperature $T_N = 5.6$ K and the critical exponent $\beta = 0.24(1)$ are obtained. Using the value of the critical exponent, the T_N of other pressures are refined. The refined T_N's are listed in Table II.

The temperature evolution of the order parameters is shown in Fig. 4. The scaled temperatures $t = T/T_N$ are used. The magnitude of the moment at each pressure is scaled by that at $t = 0.56$ which corresponds to the base temperature of the data at 1.4 GPa. The order parameters for all the pressures yield to the same curve, indicating that the universality class of the ordered phase is independent on pressure.

The obtained exponent $\beta = 0.24(1)$ is close to $\beta = 0.253$ which is the theoretical prediction for an XY stacked triangular

TABLE II. The estimated T_N and magnitude of the magnetic moment $|M|$ at each pressure.

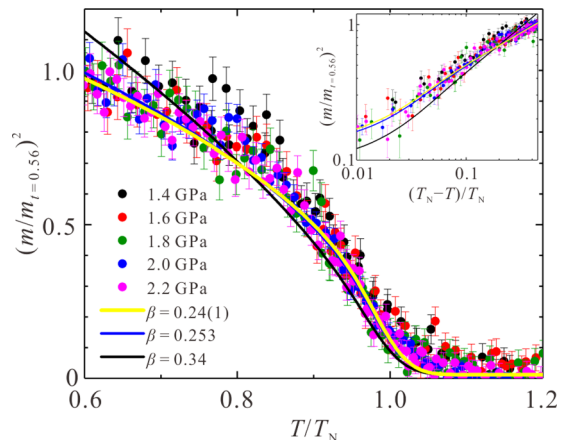| P (GPa)	T_N (K)	$\|M\|$ (μ_B)	R_F (%)
1.4	2.8	2.63(4)	7.23
1.6	3.8	2.87(5)	7.62
1.8	4.5	3.10(6)	10.1
2.0	4.7	3.16(5)	7.63
2.2	5.6	3.15(2)	3.47

FIG. 4. Temperature evolution of the order parameter for each pressure. The temperatures are scaled by $t = T/T_N$. The order parameters are scaled by the magnitudes of the moments at $t = 0.56$. Yellow, blue, and black solid curves indicate calculation curves having the critical exponents β of 0.24(1), 0.253, and 0.34, respectively. The inset is the log-log of $(m/m_{t=0.56})^2$ vs $(T_N - T)/T_N$.

AF (STA) [42,43]. The temperature dependences of the order parameter using critical exponents $\beta = 0.253$ for the XY STA model and $\beta = 0.34$ for the 3D XY model [44] are indicated by the blue and black solid curves in Fig. 4. The parameters other than β are the same as those at 2.2 GPa. Compared with the theoretical curves, the XY STA model is more reasonable than the 3D XY model. Considering the lattice symmetry and the strong easy-plane anisotropy [33], we can safely conclude that the universality class in CsFeCl3 belongs to the XY STA model. So far, the universality class of the Heisenberg or XY STA model has been reported in CsMnBr3 [$\beta = 0.25(1)$] [45], CsCuCl3 [$\beta = 0.25(2)$] [46], and CsNiCl3 [$\beta = 0.243(5)$] [47] even though all of them exhibit the magnetic long-range order already at ambient pressure, suggesting the absence of pressure-induced QPT, and inaccessibility to the QCP.

The XY STA model is characterized by the continuous $U(1)$ and discrete Z_2 symmetries, i.e., $U(1) \times Z_2$ symmetry [42,43]. In this symmetry, it is predicted that a chiral liquid state [31,48,49], in which only the Z_2 symmetry is broken and the vector chirality $\kappa_{ij} = S_i \times S_j$ is ordered, emerges on the side of the quantum disordered phase. The chiral liquid state can be detected by the measurement of dielectric property because the vector chirality is related to magnetoelectric effect based on the spin current mechanism [50–52]. The chiral liquid state in the XY STA model has not been observed in CsMnBr3, CsCuCl3, and CsNiCl3, which exhibit the magnetic long-range order at ambient pressure. CsFeCl3 is thus a candidate that is accessible to the chiral liquid state in the vicinity of the QCP in the disordered phase.

In conclusion the 120° structure with the propagation vector of $k_{mag} = (1/3, 1/3, 0)$ was evidenced in the pressure-induced ordered phase of CsFeCl3 by the combination of the neutron diffraction experiments under pressures and magnetic structure analysis. The critical exponent of the order parameter was estimated to be $\beta = 0.24(1)$, which was consistent with that for the XY STA model $\beta = 0.253$. This criticality belongs to

the universality class $U(1) \times Z_2$ in which the chiral liquid state is predicted. The study on the spin dynamics under pressure has a chance to observe a nontrivial magnon in the vicinity of the QCP in the frustrated triangular lattice for a future perspective.

[1] S. Sachdev, *Quantum Phase Transitions*, 2nd ed. (Cambridge University Press, Cambridge, UK, 2011).

[2] S. Sachdev, Science **288**, 475 (2000).

[3] A. Koga and N. Kawakami, Phys. Rev. Lett. **84**, 4461 (2000).

[4] T. Giamarchi, Ch. Rüegg, and O. Tchernyshyov, Nat. Phys. **4**, 198 (2008).

[5] E. Dagotto, Rev. Mod. Phys. **66**, 763 (1994).

[6] J. Orenstein and A. J. Millis, Science **288**, 468 (2000).

[7] J. Paglione and R. L. Greene, Nat. Phys. **6**, 645 (2010).

[8] T. Shibauchi, A. Carrington, and Y. Matsuda, Annu. Rev. Condens. Matter Phys. **5**, 113 (2014).

[9] P. Gegenwart, Q. Si, and F. Steglich, Nat. Phys. **4**, 186 (2008).

[10] Q. Si and F. Steglich, Science **329**, 1161 (2010).

[11] B. Spivak, S. V. Kravchenko, S. A. Kivelson, and X. P. A. Gao, Rev. Mod. Phys. **82**, 1743 (2010).

[12] M. Greiner, O. Mandel, T. Esslinger, T. W. Hänsch, and I. Bloch, Nature (London) **415**, 39 (2002).

[13] I. Bloch, J. Dalibard, and W. Zwerger, Rev. Mod. Phys. **80**, 885 (2008).

[14] A. Oosawa, M. Ishii, and H. Tanaka, J. Phys.: Condens. Matter **11**, 265 (1999).

[15] H. Tanaka, A. Oosawa, T. Kato, H. Uekusa, Y. Ohashi, K. Kakurai, and A. Hoser, J. Phys. Soc. Jpn. **70**, 939 (2001).

[16] A. Oosawa, M. Fujisawa, T. Osakabe, K. Kakurai, and H. Tanaka, J. Phys. Soc. Jpn. **72**, 1026 (2003).

[17] K. Goto, M. Fujisawa, T. Ono, H. Tanaka, and Y. Uwatoko, J. Phys. Soc. Jpn. **73**, 3254 (2004).

[18] Ch. Rüegg, A. Furrer, D. Sheptyakov, Th. Strässle, K. W. Krämer, H.-U. Güdel, and L. Mélési, Phys. Rev. Lett. **93**, 257201 (2004).

[19] P. Merchant, B. Normand, K. W. Krämer, M. Boehm, D. F. McMorrow, and Ch. Rüegg, Nat. Phys. **10**, 373 (2014).

[20] T. Nikuni, M. Oshikawa, A. Oosawa, and H. Tanaka, Phys. Rev. Lett. **84**, 5868 (2000).

[21] M. Matsumoto, B. Normand, T. M. Rice, and M. Sigrist, Phys. Rev. B **69**, 054423 (2004).

[22] A. Khudoyberdiev, A. Rakhimov, and A. Schilling, New J. Phys. **19**, 113002 (2017).

[23] Y. Kulik and O. P. Sushkov, Phys. Rev. B **84**, 134418 (2011).

[24] Y. Q. Qin, B. Normand, A. W. Sandvik, and Z. Y. Meng, Phys. Rev. Lett. **118**, 147207 (2017).

[25] J. Oitmaa, Y. Kulik, and O. P. Sushkov, Phys. Rev. B **85**, 144431 (2012).

[26] S. Jin and A. W. Sandvik, Phys. Rev. B **85**, 020409(R) (2012).

[27] M.-T. Kao and F.-J. Jiang, Eur. Phys. J. B **86**, 419 (2013).

[28] D.-R. Tan and F.-J. Jiang, Phys. Rev. B **95**, 054435 (2017).

[29] H. D. Scammell and O. P. Sushkov, Phys. Rev. B **95**, 094410 (2017).

[30] M. Matsumoto and M. Koga, J. Phys. Soc. Jpn. **76**, 073709 (2007).

[31] Z. Wang, A. E. Feiguin, W. Zhu, O. A. Starykh, A. V. Chubukov, and C. D. Batista, Phys. Rev. B **96**, 184409 (2017).

[32] A. Kohne, E. Kemnitz, H. Mattausch, and A. Simon, Z. Kristallogr. **203**, 316 (1993).

[33] H. Y. W. Kozukue and K. Hirakawa, J. Phys. Soc. Jpn. **49**, 144 (1980).

[34] P. A. Montano, H. Shechter, E. Cohen, and J. Makovsky, Phys. Rev. B **9**, 1066 (1974).

[35] N. Kurita and H. Tanaka, Phys. Rev. B **94**, 104409 (2016).

[36] J. Rodriguez-Carvajal, Physica B **192**, 55 (1993).

[37] A. S. Wills, Physica B **276-278**, 680 (2000).

[38] H. Nakao, M. Nishi, Y. Fujii, T. Masuda, I. Tsukada, K. Uchinokura, K. Hirota, and G. Shirane, J. Phys. Soc. Jpn. **68**, 3662 (1999).

[39] Y. J. Wang, V. Kiryukhin, R. J. Birgeneau, T. Masuda, I. Tsukada, and K. Uchinokura, Phys. Rev. Lett. **83**, 1676 (1999).

[40] D. M. Pajerowski, C. R. Rotundu, J. W. Lynn, and R. J. Birgeneau, Phys. Rev. B **87**, 134507 (2013).

[41] M. G. Kim, M. Wang, G. S. Tucker, P. N. Valdivia, D. L. Abernathy, S. Chi, A. D. Christianson, A. A. Aczel, T. Hong, T. W. Heitmann, S. Ran, P. C. Canfield, E. D. Bourret-Courchesne, A. Kreyssig, D. H. Lee, A. I. Goldman, R. J. McQueeney, and R. J. Birgeneau, Phys. Rev. B **92**, 214404 (2015).

[42] H. Kawamura, J. Phys. Soc. Jpn. **61**, 1299 (1992).

[43] H. Kawamura, J. Phys.: Condens. Matter **10**, 4707 (1998).

[44] M. Campostrini, M. Hasenbusch, A. Pelissetto, P. Rossi, and E. Vicari, Phys. Rev. B **63**, 214503 (2001).

[45] Y. Ajiro, T. Nakashima, Y. Unno, H. Kadowaki, M. Mekata, and N. Achiwa, J. Phys. Soc. Jpn. **57**, 2648 (1988).

[46] U. Schotte, N. Stusser, K. D. Schotte, H. Weinfurter, H. M. Mayer, and M. Winkelmann, J. Phys.: Condens. Matter **6**, 10105 (1994).

[47] M. Enderle, R. Schneider, Y. Matsuoka, and K. Kakurai, Physica B **234**, 554 (1997).

[48] A. V. Chubukov and O. A. Starykh, Phys. Rev. Lett. **110**, 217210 (2013).

[49] E. Parker and L. Balents, Phys. Rev. B **95**, 104411 (2017).

[50] H. Katsura, N. Nagaosa, and A. V. Balatsky, Phys. Rev. Lett. **95**, 057205 (2005).

[51] I. A. Sergienko and E. Dagotto, Phys. Rev. B **73**, 094434 (2006).

[52] M. Mostovoy, Phys. Rev. Lett. **96**, 067601 (2006).